Synthesis and Growth Discussion of One-Dimensional MgO Nanostructures: Nanowires, Nanobelts, and Nanotubes in VLS Mechanism

Youguo Yan,*,†,‡ Lixia Zhou,† Jun Zhang,† Haibo Zeng,‡ Ye Zhang,‡ and Lide Zhang‡

College of Physical Science and Technology, China University of Petroleum, 257061 Dongying, Shandong, People's Republic of China, and Key Laboratory of Materials Physics, Anhui Key Laboratory of Nanomaterials and Nanotechnology, Institute of Solid State Physics, Chinese Academy of Sciences, P.O. Box 1129, 230031 Hefei, Anhui, People's Republic of China

Received: December 29, 2007; Revised Manuscript Received: April 23, 2008

Three kinds of one-dimensional (1D) MgO nanostructures: nanowires, nanobelts, and nanotubes were synthesized through introducing the low-melting point mental Sn as catalyst in the chemical vapor deposition route. The morphology and crystalline structure were characterized by X-ray diffraction, field emission scanning electron microscopy, and transmission electron microscopy. The detailed growth processes of these structures were discussed. A conventional VLS mechanism, explicated VLS mechanism, and VLS mechanism combined with second evaporation-oxidation process were proposed to explain the growth of nanowire, nanobelt, and nanotube, respectively. The establishment of growth models on nanobelt and nanotube gave a new annotation of VLS mechanism different with previous reports, and the growth analyses are helpful to comprehensively understand VLS mechanism. These results have important referenced significance in fabrication of various 1D nanostructures. Furthermore, the obtained nanostructures may find various applications as functional building blocks in nanodevices.

1. Introduction

One-dimensional (1D) nanomaterials in form of tubes, wires, and belts have attracted much attention in the past decade because of their interesting geometries, novel properties, and potential applications.[1–3] Many material systems including carbon,[1,4] semiconductors,[2,5] oxides,[3,6] nitrides,[7] and carbides[8] have been successfully fabricated by various methods via different growth models. Among them, the VLS mechanism generally plays a key role in the synthesis of various 1D nanostructures, which was first proposed by Wagner and Ellis in 1964 for Si-whisker growth,[9] has been widely used to guide the growth of a wide range of nanowires, for example, Group IV (e.g., Si and Ge),[10] III−V (e.g., GaAs and InP),[11,12] and II−VI (e.g., ZnS and ZnSe) semiconductors,[11,13] and oxides (e.g., ZnO and SiO2).[14–16] In addition, Erik et al. also synthesized the InP nanotubes under VLS mechanism through controlling the diffusion-limited process at high temperature.[17] Gao et al. obtained In_2O_3 nanobelts using Au as catalyst.[18]

In traditional VLS, the noble metals, such as Au and Ag, are commonly employed as the catalyst to induce the growth of 1D nanostructures. Recently, many low melting point metals, such as Ga, In, Sn, Zn, etc., are also found to possess catalytic capability in the growth of 1D nanostructures.[19] A typical example is the work of Pan et al., i.e., catalyzed growth of a bundle of SiO_2 nanowires from a melt Ga microsphere; as another successful example,[19a] Professor Wang synthesized the ZnO nanopropellers using the melt Sn as catalyst.[20] The VLS mechanism is a common route to growth of 1D nanostructure. Up to now, although abundant researches in theory and experiment have been performed, there are further works, i.e., perfection of theory and exploration of structure synthesis, to be demanded for the development of nanoscience and nanotechnology.

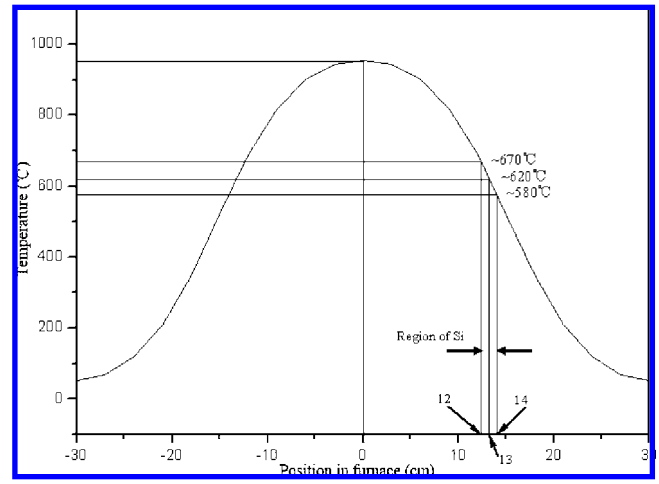

Figure 1. Temperature distributing curve in the furnace.

In this article, through controlling the reacting temperature and adoption of metal tin in the source, we designed and synthesized MgO 1D nanostructures: nanowires, nanobelts, and nanotubes in horizontal furnace. On the basis of the characterized results and previous reports about the VLS mechanism, three kinds of growth models, including a conventional VLS mechanism, explicated VLS mechanism, and VLS combined with second evaporation-oxidation process, were proposed to explain the formation of nanowire, nanobelt, and nanotube, respectively. The results and discussions enriched the synthesis science in aspects of experiment and theory. In experiment, the low melting point metal Sn was first used to synthesize these three kinds of 1D MgO nanostructures; in theory, the proposed

* To whom correspondence should be addressed. E-mail: yyg@issp.ac.cn.
† China University of Petroleum.
‡ Chinese Academy of Sciences.

10.1021/jp712149g CCC: $40.75
Published on Web 06/21/2008

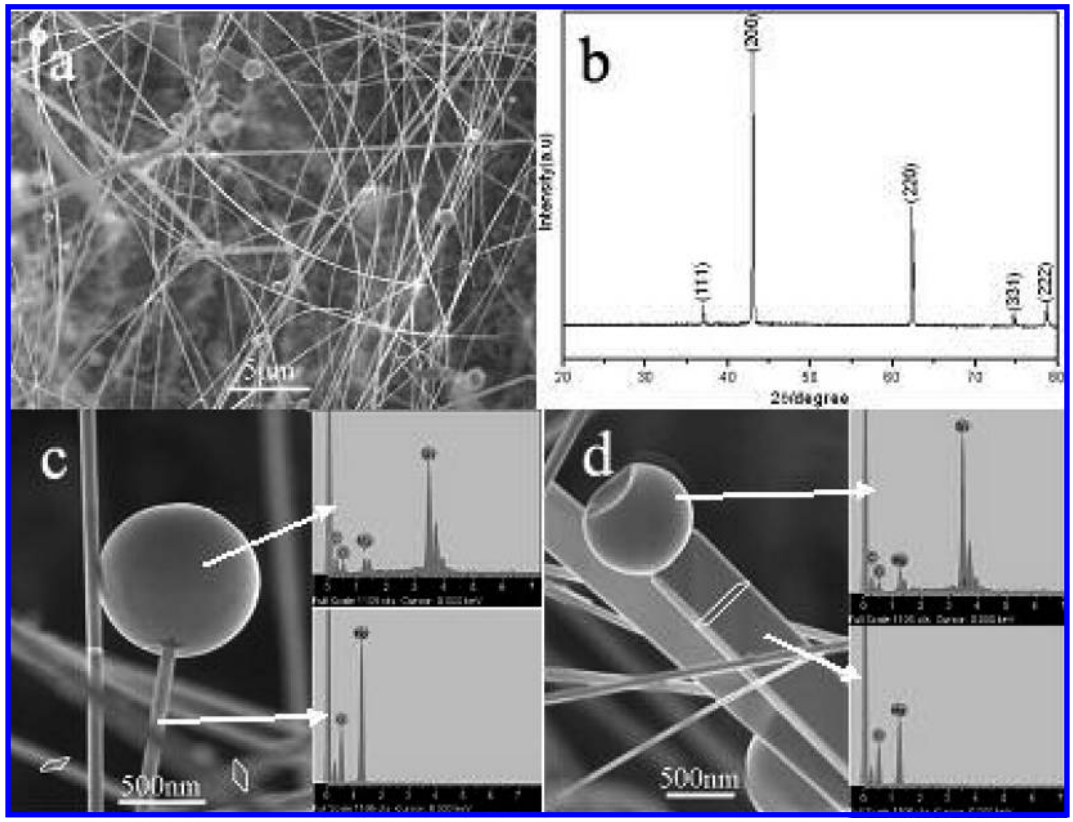

Figure 2. SEM images and XRD pattern of the sample: (a) low-magnification SEM image; (b) XRD pattern; (c,d) high-magnification SEM image of nanowire and nanobelt, respectively. The insets in panels c and d reveal the EDS patterns on the tip and body signed by white arrows, respectively.

growth models enriched and developed the conventional VLS mechanism. Furthermore, these three kinds of MgO nanostructures may look potentional future as functional building blocks in future nanodevices.

2. Experimental Sections

The synthesis of MgO nanostructures was carried out in a conventional high-temperature horizontal tube furnace. The local temperature distribution curve in the tube furnace has been calibrated in advance as shown in Figure 1. An alumina tube, 25 mm in inner diameter, was installed in the furnace. A ceramic boat loaded with a mixture of MgO, C, and Sn powder (1 g, molar ratio is 1:1:0.2) was inserted into the central heating zone of the alumina tube, and a silcon wafer (10×20 mm^2) was placed downstream to collect the products; the distance of two centers of Si wafer and the heating zone is about 13 cm. Before heating, 200 sccm Ar (purity: 99.99%) was introduced into the tube chamber for 30 min to purge the system. Afterward, the flow rate was adjusted to 50 sccm. The furnace was rapidly heated to 950 °C and kept at that temperature for 1 h. From Figure 1, it can be seen that the temperature of substrate was in the range of 580−670 °C, which was higher than the melting point of Sn (232 °C). In other words, the Sn would be at liquid phase and could induce the growth of 1D nanostructure as catalyst. After reaction, a layer of white wool-like products were found deposited onto the Si substrate.

The structure and morphology were characterized by X-ray diffraction (XRD) spectra (Philips X'pert-PRO, Cu Kα (0.15419nm) radiation), field emission scanning electronic microscope (SEM, Sirion 200 FEG) installed with energy dispersive spectroscopy (EDS, Oxford), high-resolution TEM (HRTEM, JEOL2010 at 200 kV) installed with energy dispersive spectroscopy (EDS, Oxford).

3. Results and Discussions

3.1. Characterization. The SEM image (Figure 2a) demonstrates that bulk of wire- and beltlike nanostructures were deposited onto the surface of Si substrate. There exists a large-sized sphere on the tip of each nanowire or nanobelt. The XRD spectrum of these structure corresponds to the cubic structure of MgO (JCPDS card: 4500946) with the lattice parameter $a =$ 0.421nm (Figure 2b). A magnified SEM image of the nanowire is given in Figure 2c. It can be seen that a finer nanowire with diameter of about 80 nm is terminated with a large-sized catalyst particle (~900 nm in diameter). Detailed observation indicates that the obtained nanowire possess semisquare cross-section (signified with white pane). The EDS spectra on different sites (the catalyst particle and the body of nanowire) give the correlative information of component ratio (Figure 2c). In the catalyst particle, the atomic ratio of Sn/Mg/O/C is 23.56:4.58:33.18:38.68. In the nanowire, the EDS indicates the atomic ratio of Mg/O is 44.52:55.48. It reveals that the obtained nanowire was composed of MgO. From these two EDS results, we can conclude that the growth of MgO nanowire initiates from the eutectic alloy droplet Sn−Mg−O through VLS growth mechanism. The high-magnification SEM image (Figure 2d) of the nanobelt shows that the nanobelt possesses a quadrate cross section with width thickness ratio about 5 and is ended by a faulty sphere with sunken tip. The component ratio in the catalyst particle (Sn/Mg/O/C = 32.57:5.02:30.25:32.16) and nanobelt (Mg/O = 43.65:56.35) as revealed by EDS spectra demonstrates that the nanobelt is MgO. Above results also

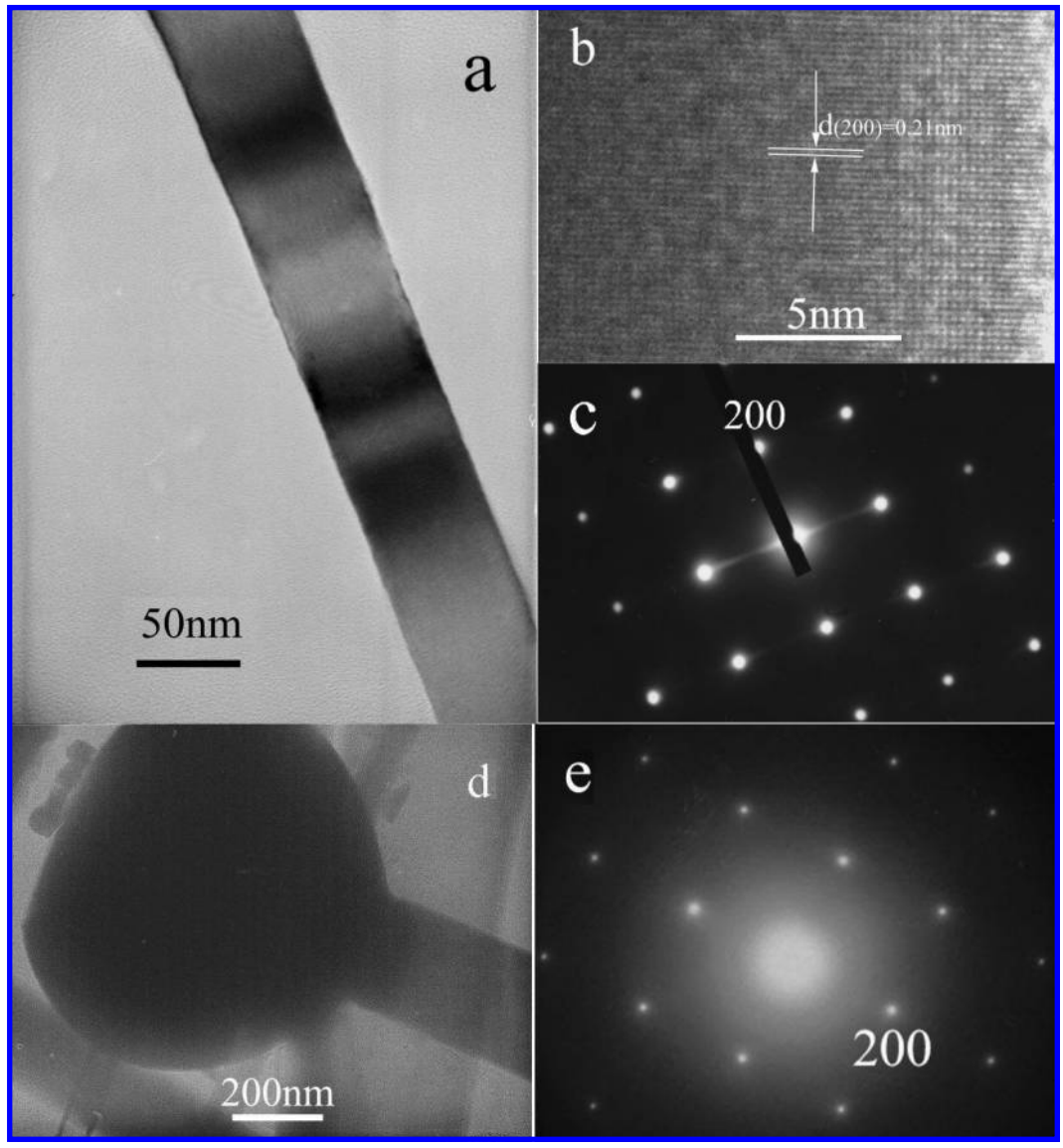

Figure 3. TEM image of the nanowire and nanobelt: (a,d) low-magnification TEM images of nanowire and nanobelt, respectively; (b,c) high-magnification lattice image and SAED of nanowire; (e) SAED image of nanobelt.

indicate that the growth of MgO nanobelt was catalyzed by the eutectic Sn−Mg−O alloy droplets under VLS mechanism.

The microstructure of as-prepared sample was characterized by TEM and electron diffraction (ED). Figure 3a displays a low-magnification TEM image of a typical MgO nanowire with uniform size about 65 nm. HRTEM image (Figure 3b) reveals the planar spacing along the growth direction is 0.21 nm, which corresponds to the spacing of (200) plane of MgO cubic structure. The information is also verified by the SAED (Figure 3c). The low-magnification TEM image of the nanobelt is given in Figure 3d. It can be seen that a nanobelt grows from the bottom of an ellipsoidal particle with a truncated top plane. The SAED (Figure 3g) perpendicular to the nanobelt reveals the axial growth is along [100].

Two other structures, short tubular nanostructure ended with a large-sized nanoparticle (Figure 4a) and long nanotubes (Figure 4b), were also visualized by TEM. The short nanotube and long nanotube possess almost the same diameter implying that these two kinds of nanotubes may have originated from a united structures. The separation of the body and the tip may be owing to the ultrasonic treatment in the preparation of TEM sample. The SAED pattern as shown in inset of Figure 4b demonstrates that the nanotube possessed a polycrystalline structure. The EDS also confirmed the element component. Figure 4c gives the atomic raito (Sn/Mg/O/C = 17.56:18.58:30.18:33.68) in the topmost particle; Figure 4d reveals that the atomic ratio of Mg/O/C is 28.41:54.35:17.24, which implies the MgO structure of nanotube. Above results indicated the growth of MgO nanotube was induced by the eutectic droplet Sn−Mg−O.

3.2. Analysis of Growth Mechanism. It is emphasized that the liquid droplet is a unique characteristic of VLS growth. As to the MgO nanowires, nanobelts, and nanotubes, there exists a catalyst particle on their tip, so the VLS mechanism surely is involved in the growth of these three kinds of nanostructures. Therfore, three different growth models related to VLS mechanism were proposed to explain their growth as shown in Figure 5.

3.2.1. Nanowires. As to the nanowire, the growth can be ascribed to the traditional VLS mechanism. The growth process is composed of four steps as shown in Figure 5a. First, in the initial stage, the Sn first vaporized then was transported downstream and condensed into small droplet on the surface of the substrate. Second, with the increasing of reacting

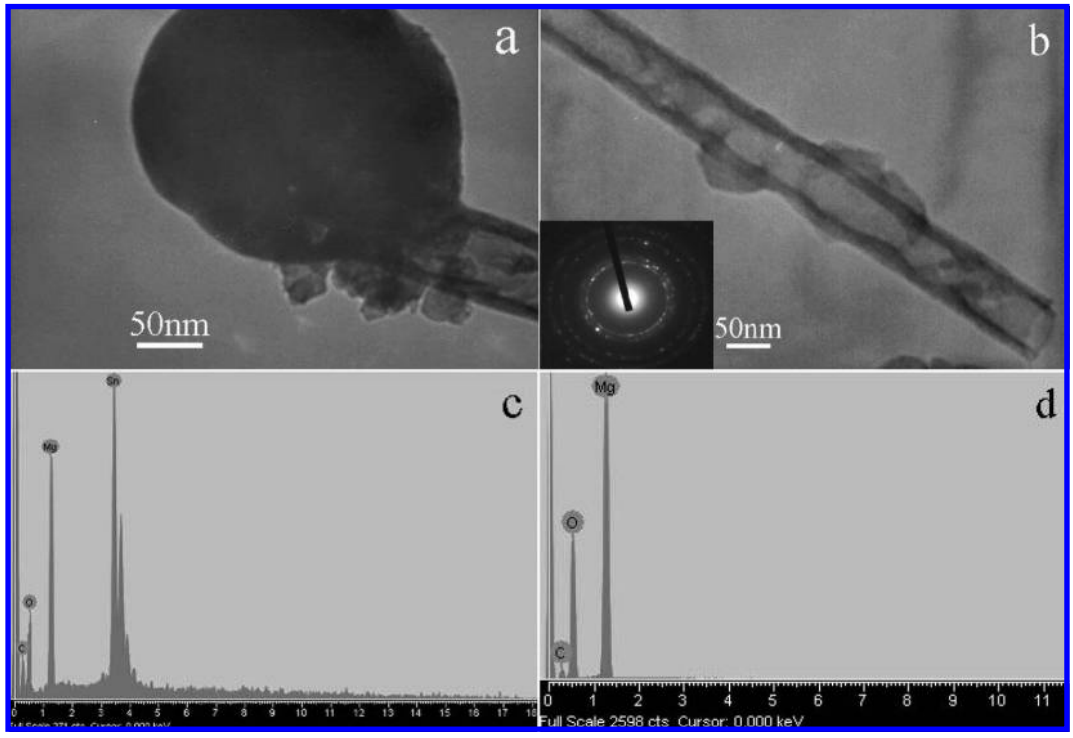

Figure 4. TEM images, SAED and EDS patterns of nanotube: (a,b) TEM images of tip and body of the nanotube, respectively; the inset in panel b gives the SAED pattern on the wall of tube. (c,d) EDS patterns of the catalyst particle and the wall of nanotube.

temperature, the Mg vapor would be yielded through carbon thermal reduction of MgO and C. Simultaneously, the Mg vapor would react with oxygen to form MgO molecules. The reagent species Mg and oxygen in phase would preferentially adsorb onto the surface of Sn droplet and formed the Sn−Mg−O eutectic alloy droplet; the oxygen may come from the residue and leakage of the reaction system. Third, continuous dissolution of Mg, O, and MgO molecules into the droplets would lead to the supersaturation of reagent; then the nucleation and growth of MgO nanowires occurred, and the square cross section of MgO nanowire was related to the crystal symmetry of cubic MgO. Finally, the nanowire growth would continue until the catalyst alloy did not remain in a liquid state or the reactant is exhausted in the end of reaction.[21]

3.2.2. Nanobelts. There are two viewpoints to be employed to explain the fact that nanobelt is terminated by a catalytic particle: First, Li et al. considered that the growth behavior of nanobelts were different from that of the conventional nanowire growth under VLS mechanism. The catalyst droplet was only involved in the physical absorption process rather than contributing to the further growth of 1D naostructure, and the temperature was an important parameter affecting the nanobelt morphology. In this viewpoint, the low temperature would be in favor of the growth of nanowire, while the high temperature would lead to the formation of nanobelt.[22] Second, Gao et al. proposed a model of axial VLS growth and side VS growth.[23] This explanation was also adopted by Hao to explain the growth of ZnS nanobelt.[24] In previous reports, the obtained nanobelts with catalyst particle mostly have similar character: tapered tip with decreasing width, while the MgO nanobelt obtained in our experiment has uniform width from tip to bottom, which cannot be well explained by the above two viewpoints. As to the first one, they consider that the synthesized temperature of nanowires and nanobelts is different, which was not in accord with the uniform distribution of nanowires and nanobelts on the whole substrate, which have a temperature distributing grads. As for the second viewpoint, the tapered tip was a typical symbol of side growth, which failed to meet with the uniform size of nanobelt in our sample. As to the MgO nanobelt in our experiment, we proposed an interface concept to explain the growth of nanobelt different with the growth of nanowire under classical VLS mechanism, defined as explicated VLS mechanism.

In the VLS, the configuration of the catalyst particle always has an important affect on the cross-section of the catalyzed 1D nanostructure. From Figure 2a, it can be seen that the growth of nanobelts was mostly induced by the faulty spherical particle with truncated tip, as shown in Figure 2b. As to the formation of faulty sphere, we consider that the faulty sphere originated from more than two adjacent smaller Sn droplets, which had definite probability to link together when their size became large during heating. Hereby, we proposed following growth process.

In the heating stage, the Sn power vaporized and formed small droplets on the substrate. The size of the droplets gradually becomes large with continuous dissolution of coming Sn vapor. With the size increase of Sn droplet, the adjacent Sn droplets with especially small interval would have a definite possibility of linking together. The linked droplets would further grow and evolve into a large sphere. During the evolution, the interface would go through a medial procedure and have an elliptical interface, which would induce the growth of nanobelt. On the basis of this model, the different width-to-thickness ratio could be ascribed to the different number of linked adjacent catalyst droplets, i.e., more linked droplets would lead to the formation of a broad nanobelt with large width-to-thickness ratio, while, the few linked droplets would lead to the growth of a narrow nanobelt with small width-to-thickness ratio. If the growth was induced by a single droplet, the obtained nanostructure would be a nanowire with a square cross-section as described above.

Figure 5b gives a typical growth sketch map of nanobelt induced by two linked Sn droplet. Step I was the formation of two separated Sn droplets on the substrate, and the interface with the silicon substrate was two individual circular planes.

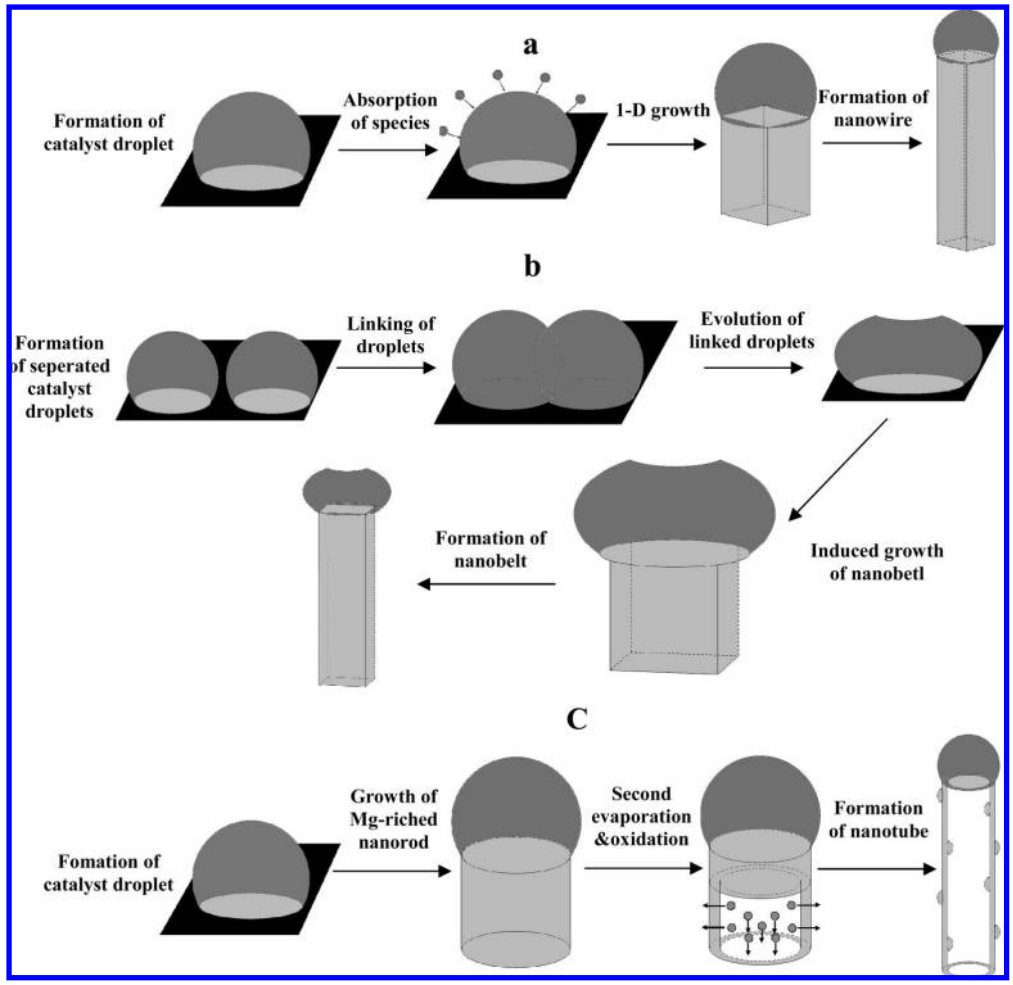

Figure 5. The growth sketch map of the nanowire, nanobelt, and nanotube. (a) Growth process of nanowire: formation of catalyst droplet → absorption of reagent → 1D growth → formation of nanowire. (b) Growth process of nanobelt: formation of separated catalyst droplets → linking of droplets → evolution of linked droplets → induced growth of nanobelt → formation of nanobelt. (c) Growth process of nanotube: formation of catalyst droplet → growth of Mg-riched nanorod → second evaporation and oxidation → formation of nanotube.

At step II, the two Sn droplets became large and linked together, and the interface was two linked circular planes. At step III, the linked droplets further grew and formed an ellipsoidal sphere, and the interface was semielliptic plane; the elliptic plane would act as preferentially nucleated sites and induced the growth of nanobelts with rectangular cross section, which was in accord with the cubic crystal symmetry of MgO. At step IV, the growth would continue until the catalyst alloy did not remain in liquid state or the reactant was exhausted in the end of reaction.

3.2.3. Nanotube. As to the formation of tubular structure under VLS mechanism, the related reports are few. A broad accepted growth model was proposed by Erick et al. in which they considered that the formation of hollow nanotube can be ascribed to the diffusion limit in the droplet at high temperature, which results in ring-shaped nucleation and induced the growth of nanotube.[17]

Detailed observation (Figure 4a,b) indicated that there existed some absorbed particles on the inner and outer wall of the tube, and more particles were found on the linked part between the catalyzed particle and the body of tube. On the basis of this information, we proposed a VLS combined with second evaporation-oxidation process to explain the formation of MgO nanotube in our experiment (Figure 5c).

In the initial stage of reaction, the eutectic alloy droplet first formed on the surface of the substrate. Comparing the EDS results of catalyst droplets in nanowire, nanobelt, and nanotube, it can be seen that the atomic ratio of Mg in nanotube was much higher than the nanowire and nanobelt. The higher atomic ratio of Mg in the eutectic droplet would result in the formation of Mg-enriched nanorod. Under high growing temperature (580−670 °C), a second evaporationand oxidation of Mg in the nanorod would go on and form tubular structure. The volatilized Mg vapor would dissipate from the bottom nozzle and the wall of tube, which affirmatively resulted in the adsorption of the particle on the outer and inner wall of the nanotube, which was in accord with TEM results. Meanwhile, the growth of new Mg-enriched nanorod would continue. Above processes were repeated and finally formed nanotube.

3.2.4. Comparisons of These Three Growth Models. Through the analysis of these three kinds of 1D MgO nanostructures, it could be seen that the VLS mechanism was the primary growth mode, and the morphology discrimination was determined by the configuration and component in the catalyst particle. The single Sn droplet would induce the growth of nanowire with square cross section, and the linked Sn droplets would induce the growth of nanobelt with rectangular cross section. As for the nanotube, the formation of Mg-enriched nanorod and following evaporation and oxidation answered for the formation of tubular nanostructure, which was determined by the high Mg atomic ratio in catalyst droplet and growth temperature.

The yield was an important index in synthesis science, which determined the application value of synthesized nanostructure. In our sample, from the SEM image it could be seen that the yield of nanowires is large (~90%_, while the yield of nanobelt was relatively less (~10%). As to the nanotube, the yield was less; these kinds of structures were only found in the TEM observation accidentally.

4. Conclusions

In summary, three kinds of 1D MgO nanostructures, nanowires, nanobelts and nanotubes, were synthesized using Sn as catalyst through chemical vapor deposition route. XRD, SEM, and TEM were used to characterize the morphology and crystalline structure. The growth processes of these three kinds of structures were discussed in depth and three distinct growth models were proposed based on the characterized results. First, as to nanowire, the growth could be explained by the traditional VLS mechanism, i.e., an individual Sn alloy droplet induced the growth of single nanowire with square cross section, and the interface of catalyst droplet and substrate was a circular plane. Second, the growth of nanobelt was induced by an ellipsoidal catalyst droplet and had an elliptic interface with the substrate. The formation of ellipsoidal catalyst droplet could be ascribed to the combination of two or more adjacent catalyst droplets. The formation of nanotube under VLS mechanism could be divided into two steps: first, the Mg-enriched nanorod that formed was induced by the catalyst droplet with higher Mg atomic ratio than that of nanowire and nanobelt; second, the evaporation and oxidation of Mg-enriched nanorod would result in the formation of tubular structure. Our analysis elucidated three different growth models under VLS mechanism, and the research results and discussions enriched and developed the synthesis science in aspects of experimental exploration and theoretic perfection. Moreover, the obtained three kinds of MgO nanostructures have potential applications as functional building blocks for fabricating nanodevices.

Acknowledgment. This work was financially supported by the National Major Project of Fundamental Research: Nanomaterials and Nanostructures (Grant 2005CB23603), the Special Fund for President Scholarship, Chinese Academy of Sciences, and the National Natural Science Foundation of China (Grant 90406008).

References and Notes

(1) Iijima, S. *Nature* **1991**, *354*, 56.
(2) Morales, A.; Lieber, C. M. *Science* **1998**, *279*, 208.
(3) Pan, Z. W.; Dai, Z. R.; Wang, Z. L. *Science* **2001**, *291*, 1947.
(4) (a) Pan, Z. W.; Xie, S. S.; Chang, B. H.; Wang, C. Y.; Lu, L.; Liu, W.; Zhou, W. Y.; Li, W. Z.; Qian, L. X. *Nature* **1998**, *394*, 631. (b) Fan, S. S.; Chapline, M. G.; Franklin, N. R.; Tombler, T. W.; Cassell, A. M.; Dai, H. J. *Science* **1999**, *283*, 512.
(5) (a) Pan, Z. W.; Dai, Z. R.; Xu, L.; Lee, S. T.; Wang, Z. L. *J. Phys. Chem. B* **2001**, *105*, 2507. (b) Wang, D. W.; Dai, H. J. *Angew. Chem., Int. Ed.* **2002**, *41*, 4783.
(6) (a) Yang, P. D.; Lieber, C. M. *J. Mater. Res.* **1997**, *12*, 2981. (b) Lao, J. Y.; Wen, J. G.; Ren, Z. F. *Nano Lett.* **2002**, *2*, 1287. (c) Zhu, Y. Q.; Hsu, W. K.; Terrones, M.; Grobert, N.; Terrones, H.; Hare, J. P.; Kroto, H. W.; Walton, D. R. M. *J. Mater. Chem.* **1998**, *8*, 1859.
(7) (a) Han, W. Q.; Fan, S. S.; Li, Q. Q.; Hu, Y. D. *Science* **1997**, *277*, 1287. (b) Chen, C. C.; Yeh, C. C.; Chen, C. H.; Yu, M. Y.; Liu, H. L.; Wu, J. J.; Chen, K. H.; Chen, L. C.; Peng, J. Y.; Chen, Y. F. *J. Am. Chem. Soc.* **2001**, *123*, 2791.
(8) (a) Dai, H. J.; Wong, E. W.; Lu, Y. Z.; Fan, S. S.; Lieber, C. M. *Nature* **1995**, *375*, 769. (b) Pan, Z. W.; Lai, H. L.; Au, F. C. K.; Duan, X. F.; Zhou, W. Y.; Shi, W. S.; Wang, N.; Lee, C. S.; Wong, N. B.; Lee, S. T. *Adv. Mater.* **2000**, *12*, 1186.
(9) Wagner, R. S.; Ellis, W. C. *Appl. Phys. Lett.* **1964**, *4*, 89.
(10) Morales, A. M.; Lieber, C. M. *Science* **1998**, *279*, 208.
(11) Duan, X. F.; Lieber, C. M. *Adv. Mater.* **2000**, *12*, 298.
(12) Gudiksen, M. S.; Wang, J. F.; Lieber, C. M. *J. Phys. Chem. B* **2001**, *105*, 4062.
(13) Wang, Y. W.; Zhang, L. D.; Liao, C. H.; Wang, G. Z.; Peng, S. S. *Chem. Phys. Lett.* **2002**, *357*, 314.
(14) Huang, M. H.; Wu, Y. Y.; Feick, H.; Tran, N.; Weber, E.; Yang, P. D. *Adv. Mater.* **2001**, *13*, 113.
(15) Huang, M. H.; Mao, S.; Feick, H.; Yan, H. Q.; Wu, Y. Y.; Kind, H.; Weber, E.; Russo, R.; Yang, P. D. *Science* **2001**, *292*, 1897.
(16) Pan, Z. W.; Dai, Z. R.; Ma, C.; Wang, Z. L. *J. Am. Chem. Soc.* **2002**, *124*, 1817.
(17) Bakkers, E. P. A. M.; Verheijen, M. A. *J. Am. Chem. Soc.* **2003**, *125*, 3440.
(18) Gao, T.; Wang, T. H. *J. Cryst. Growth* **2006**, *290*, 660.
(19) (a) Pan, Z.; Dai, S.; Beach, D. B.; Lowndes, D. H. *Nano Lett.* **2003**, *3*, 1279. (b) Pan, Z.; Dai, S.; Beach, D. B.; Lowndes, D. H. *Appl. Phys. Lett.* **2003**, *83*, 3159. (c) Sun, S.; Meng, G.; Zhang, M.; Hao, Y.; Zhang, X.; Zhang, L. *J. Phys. Chem. B* **2003**, *107*, 13029. (d) Gao, P.; Ding, Y.; Wang, Z. *Nano Lett.* **2003**, *3*, 1315. (e) Lao, J.; Huang, J.; Wang, D.; Ren, Z. *J. Mater. Chem.* **2004**, *14*, 770. (f) Ye, C.; Zhang, L.; Fang, X.; Wang, Y.; Yan, P.; Zhao, J. *Adv. Mater.* **2004**, *16*, 1019.
(20) Gao, P. X.; Wang, Z. L. *Appl. Phys. Lett.* **2004**, *84*, 2883.
(21) Wu, Y. Y.; Yang, P. D. *J. Am. Chem. Soc.* **2001**, *123*, 3165.
(22) Li, Q.; Wang, C. R. *Appl. Phys. Lett.* **2003**, *83*, 359.
(23) Gao, T.; Wang, T. H. *J. Phys. Chem. B* **2004**, *108*, 20045.
(24) Hao, Y. F.; Meng, G. W.; Wang, Z. L.; Ye, C. H.; Zhang, L. D. *Nano Lett.* **2006**, *6*, 1650.

JP712149G